Bridging the gap across scales: coupling CFD and MD/GCMC in polyurethane foam simulation

Mohsen Karimi[*a1], *Daniele Marchisio*[a], *Erik Laurini*[b], *Maurizio Fermeglia*[b], *Sabrina Pricl*[b]

[a] *Department of Applied Science and Technology, Institute of Chemical Engineering, Politecnico di Torino, C.so Duca degli Abruzzi 24, 10129 Torino, Italy.*

[b] *Molecular Simulation Engineering (MOSE) Laboratory, Department of Engineering and Architecture (DEA), Trieste University,*

34127, Trieste, Italy.

[*] *Corresponding author: Mohsen Karimi; mohsen.karimi@polito.it; Department of Applied Science and Technology, Institute of Chemical Engineering, Politecnico di Torino, C.so Duca degli Abruzzi 24, 10129 Torino, Italy*

Abstract:

This work presents a multi-scale approach to reacting and expanding polyurethane (PU) foams modeling and simulation. The modeling strategy relies on two pillars: an atomistic model (molecular dynamics (MD)/Grand Canonical Monte Carlo (GCMC)) that provides liquid mixture density and reactant solubility and a continuum model (CFD) in which the expansion characteristics of the foam is modeled exploiting the results of the atomistic simulations. The resulting coupled model is validated for two different PU systems applied in four batches with chemical and physical blowing agents. The results demonstrate the efficacy and reliability of the developed model in the simulation of different PU foam properties such as apparent density and temperature evolutions.

Keywords: Multi-scale Modeling; Polyurethane; Computational Fluid Dynamics; Molecular Dynamics/Grand Canonical Monte Carlo; Surrogate Model

[1] Present Address: Department of Chemistry and Chemical Engineering, Chalmers University of Technology, 412 96 Gothenburg, Sweden

1. Introduction

Polyurethane (PU) foams are interesting materials employed in furniture, construction and automotive industries, just to cite a few, and represent an important share of the global polymer materials market (Mills, 1993; Princen and Kiss, 1986; Woods, 1990). PU are manufactured by mixing the two main PU components (i.e., a mixture of polyols and isocyanates) with additives. These include catalysts (to tune polymerization rate) and emulsifiers (to improve reactant compatibility). To generate gas bubbles leading to foam, physical and chemical blowing agents are employed. Physical blowing agents (PBAs) are volatile hydrocarbons that evaporate by virtue of the exothermicity of the polymerization reaction. On the other hand, the mechanism of action of chemical blowing agents (CBAs) is based on their reaction with the polymerization mixture, and ultimately results in gas production. One of the most popular CBAs is water, which reacts with isocyanates to produce carbon dioxide leading to the foam expansion.

Modeling and simulation of a PU foam expansion process is particularly interesting because, being a rapidly time-evolving system, it is very difficult to characterize experimentally. A model describing PU foam expansion, especially for mold filling applications, could be profitably used in the design and optimization of such processes. On the other hand, the scientific modeling community faces a complex multiphase-reacting system in which various physical phenomena encompassing a wide range of length scales take place. This deters scientists to face the problem as a unified challenge, while the current, practical approach is tackling the problem at each single scale (e.g., nano-, meso-, and macro-scale models). Additionally, the final properties of the manufactured PU foam highly depend on the adopted chemical recipe (i.e., polyol, isocyanate, and blowing agents structure and concentrations) and the flow history of the foam when it is applied for mold filling applications. This, in turn, requires the knowledge of fundamental thermophysical properties of different components (e.g., the density of polymerizing mixture) prior and during foam expansion for large-scale applications. Accordingly, the problem is inherently multiscale and, as such, a multi-model approach must be devised and applied.

A review of the current literature on the bubble-scale modeling tools for PU shows that one crucial point consists in correctly describing how an individual spherical bubble grows within a shell of the reacting mixture. Mass and momentum balances are routinely solved to assess the evolution of bubble radius while the mass transfer coefficient is considered as a model parameter (Feng and Bertelo, 2004; G. Harikrishnan et al., 2006; Harikrishnan and Khakhar, 2009; Kim and Youn, 2000). Furthermore, the macro-scale characteristics of PU foams are generally modeled by solving either ordinary differential equations (ODEs) or partial differential equations (PDEs). The former approach describes the foam apparent density, temperature, and polymerization progress (i.e., the gelling and blowing reactions) with respect to reaction kinetics (S. A. Baser and Khakhar, 1994; S A Baser and Khakhar, 1994; Gupta and Khakhar, 1999). Along the alternative line, Computational Fluid Dynamics (CFD) is applied to account for spatial and temporal variation of the foam properties. This last method has proven to be more attractive for mold filling applications, as the foam mobile interface can be monitored using the Volume-of-Fluid (VOF) approach (Bikard et al., 2005; Geier et al., 2009; Samkhaniani et al., 2013; Seo et al., 2003; Seo and Youn, 2005).

From a general perspective, to model PU-based systems we recently developed NANOTOOLS, an integrated, multiscale molecular modeling software for the prediction of major structural and thermophysical properties of this class of polymers and their nanocomposites (Ferkl et al., 2017; Laurini et al., 2016). Specifically, a hierarchical approach was implemented, which involves running separate models with a parametric coupling, with the ultimate goal of predicting the system under consideration from first principles, i.e. starting from the quantum scale and passing information to molecular scales and eventually to process scales. According to this sequential (aka message-passing) methodology, information is computed at a smaller (finer) scale and passed to a model at a larger (coarser) scale by leaving out (i.e. coarse graining) degrees of freedom (P Cosoli et al., 2008a; Fermeglia and Pricl, 2007; Laurini et al., 2016; Scocchi et al., 2009, 2007a, 2007b; Toth et al., 2012). On the macro-scale level, we

presented a base line model that corroborates the lack of population balance modeling for a reactive-expanding PU foam (Karimi and Marchisio, 2015). This has paved our way to implement a population balance equation (PBE) into a CFD solver and introduce a new VOF-based solver, coupled with PBE, for modeling and simulation of PU foams (Karimi et al., 2016). The results we obtained from the validation tests showed that by solving a PBE, one can extract practical information about the foam apparent density and its morphological structure. This, however, comes with the cost of compromising some physical phenomena occurring during the foam expansion, e.g., empirically driven correlations or constant values represent the characteristics of the system under investigation. For instance, we applied a simplified diffusion controlled model for the bubble growth rates. However, later we addressed this by coupling a detailed bubble-scale model with the macro-scale CFD code and showed the benefits of applying a multiscale approach on the accuracy of the numerical predictions (Ferkl et al., 2016).

The present work also follows the same philosophy outlined above. Yet, for the first time in the investigation of PU foams expansion, a macro-scale CFD model is coupled with nano-scale atomistic models. The macro-scale CFD model requires in fact three pieces of information: the density of the liquid mixture undergoing polymerization (prior to foaming), the solubility of chemical blowing agents (in the liquid mixture undergoing polymerization) and the solubility of PBA varying with temperature and degree of polymerization (or cross-linking). Accordingly, instead of using empirical and unreliable expressions for the estimation of these quantities, here the nano-scale model is employed. In particular, molecular dynamics (MD) simulations are run to calculate the density of the networking polymer (Ferkl et al., 2017; Laurini et al., 2016; Maly et al., 2008) while Grand Canonical Monte Carlo (GCMC) are carried out to predict the different gases solubility as a function of temperature and degree of cross-linking (P Cosoli et al., 2008a, 2008b; Paolo Cosoli et al., 2008; Pricl and Fermeglia, 2003). The final macro-scale CFD model predictions, calculated in turn by using results from the underpinning nano-scale models, are validated against experimental data for density and temperature time evolutions for

different test cases. The comparison shows that multiscale modeling is an extremely interesting technique for the simulation of PU foams, as it allows to describe them without the need of performing costly experiments. In fact, the most important properties affecting the final behavior of the PU foam are here calculated rather than measured. This is particularly important since not only some properties are difficult to measure, but some others are impossible to obtain experimentally in a rapidly evolving reacting system such as this one.

2. Mathematical Models

In what follows the nano- and macro-scale models will be presented. Details concerning the specific chemical systems investigated will also be summarized in this section, as they are required to lay down the nano-scale models. In the next two sections the models employed to describe a generic PU foam will be outlined. This generic PU foam is prepared by mixing polyols and isocyanates with water, producing carbon dioxide (i.e. chemical blowing agent), and a physical blowing agent. In this work, simulations are performed for two different PU recipes (labelled as Recipe 1 and Recipe 2) applied in four different PU foam batches (a to d). Recipe 1 includes a polyether polyol with an OH value = 365 mg KOH/g polyol, and polymethylene polyphenyl isocyanate with an equivalent molecular weight of 135 (Baser, 1994). Recipe 2 includes a mixture of different polyols with OH value = 370 mg KOH/g polyol and a mixture of MDI (4,4'-methylene diphenyl diisocyanate) and TDI (toluene-2,4-diisocyanate)(Geier et al., 2009). Water is used in Recipe 1 as the CBA, whereas n-pentane acts as PBA in Recipe 2. The nano-scale model calculates the density of the liquid mixture undergoing polymerization and the solubility of the physical and chemical blowing agents at different degrees of polymerization or cross-linking and different temperatures. These pieces of information are then fed to surrogate models that fit the MD/GCMC generated data into algebraic expressions, and eventually passed to the macro-scale model that simulates the PU foam.

The rationale behind this strategy is that the direct and dynamic coupling between the macro-scale and nano-scale models is not viable due to the final application of the CFD model that is simulating a three-dimensional mold geometry. In other words, calling the detailed nano-scale models for all the cells of the CFD domain under different state variables (e.g., temperature and conversion of reactants) extensively increases the computational load. Hence, one must design a communication bridge between the two scales, where not only passing the data from lower-scale to the higher-scale is appreciably fast, but it also supplies accurate approximations of the macro-scale requirements. With the adoption of surrogate models, the macro-scale inputs are wrapped into different surrogate models with parameters being statically fitted to the detailed simulations and the form of surrogate models are limited to explicit algebraic expressions.

2.1. Nano-scale MD/GCMC models

To mimic the composition of Recipe 1, the polymethylene polyphenyl isocyanate was modeled as a trimer of formula $[-C_6H_3(NCO)CH_2-]_n$ with n = 3 while, for the polyol, a glycerin/polypropylene oxide-based polyol model with ideal functionality of 3 and molecular weight of 614 was prepared. For Recipe 2, while the same polyol was adopted, the two models of 4, 4'-methylene diphenyl diisocyanate (MDI) and toluene-2, 4-diisocyanate (TDI) were prepared. The geometry of each molecular model was optimized by energy minimization using the COMPASS force field (Sun, 1998), which proved to be extremely accurate in the prediction of thermophysical properties of both condensed and gas phase systems (P Cosoli et al., 2008a, 2008b, Fermeglia and Pricl, 1999a, 1999b, 1999c; Laurini et al., 2016; Mensitieri et al., 2008; Milocco et al., 2002; Pricl and Fermeglia, 2003; Toth et al., 2012). Carbon dioxide and n-pentane optimized molecules were taken from our previous work. For both recipes, the initial liquid mixture was created by placing the suitable amount of each reagent in a 3D cubic box under periodic boundary conditions. Each resulting simulation box was relaxed and equilibrated at the corresponding initial density value at 300 K by 1 ns of MD simulations in the NVT ensemble. For the

calculation of polymer density as a function of temperature and degree of cross-linking, an adapted version of our original methodology to generate atomistic models of cross-linked networks based on molecular mechanics/dynamics schemes was adopted (Maly et al., 2008). The calculation of polymer density at each condition was performed by applying the compression-decompression MD scheme proposed by Larsen (Larsen et al., 2011). For the calculation of gas solubility, the following methodology was applied. For each temperature/degree of cross-linking couple, an equilibrated frame from the corresponding MD simulation was extracted. Next, the appropriate gas molecules were added to the simulation box and the resulting system was relaxed from major molecular overlaps. Next, GCMC simulations were performed at 1 bar following the computational recipe reported in details in our previous work (P Cosoli et al., 2008a, 2008b; Paolo Cosoli et al., 2008; Pricl and Fermeglia, 2003).

2.2. Macro-scale CFD model

The macro-scale CFD model assumes that the polyurethane foam is a perfectly homogenous mixture of initial reactants. Moreover, within the VOF method the PU foam is treated, as a pseudo-fluid interacting with surrounding air. Actually, the real three-phase system (i.e., the surrounding air, the polymerizing liquid, and the gas bubbles within the liquid) is represented as a two-phase system, i.e., the surrounding air as the primary phase and liquid mixture plus air bubbles as the secondary phase. The interface capturing method applies an indicator function to differentiate the foam phase from the surrounding air. The interface is basically a transition region and in reality this region is a discontinuous step where its value is unity in the foam phase and zero for the surrounding air. The indicator function is the volume fraction of the foam, α_f, and it obeys the continuity equation with the following form:

$$\frac{\partial \alpha_f}{\partial t} + \nabla \cdot \left(\alpha_f \mathbf{U}\right) = 0 \qquad \text{Eq. 1}$$

where $\mathbf{U}$ is the mixture velocity shared between the phases and the summation of volume fractions in each computational cell is unity (i.e., $\alpha_f + \alpha_g = 1$). Using such an approach results in the local density of the mixture to be $\rho = \alpha_f \rho_f + \left(1 - \alpha_f\right)\rho_a$. An explicit scheme is applied for the discretization of volume fraction equation in conjunction with the CICSAM (Compressive Interface Capturing Scheme for Arbitrary Meshes) scheme to produce a sharp interface. Further details on the derivation of CICSAM interface capturing scheme is reported elsewhere (Ubbink, 1997). The model is completed by a momentum balance equation, which is omitted here for the sake of brevity, but is formulated following the standard VOF model structure.

The kinetics of polymerization is accounted for by using two additional transport equations. The first one considers the gelling reaction (i.e., the reaction between isocyanates and polyols) by evaluating the conversion of the hydroxyl group, X_{OH}:

$$\frac{\partial}{\partial t}\left(\alpha_f \rho_f X_{OH}\right) + \nabla \cdot \left(\alpha_f \rho_f X_{OH} \mathbf{U}\right) = \alpha_f \rho_f S_{OH} \qquad \text{Eq. 2}$$

The source term for Eq. 2 reads as:

$$S_{OH} = A_{OH} \exp\left(-\frac{E_{OH}}{RT}\right) c_{OH,0}(1 - X_{OH})\left(\frac{c_{NCO,0}}{c_{OH,0}} - 2\frac{c_{W,0}}{c_{OH,0}} X_W - X_{OH}\right) \qquad \text{Eq. 3}$$

where A_{OH} and E_{OH} are the pre-exponential factor and the activation energy for the gelling reaction, respectively. The initial molar concentration of the polyol reactive groups is defined as $c_{OH,0}$, the initial molar concentration of isocyanate groups is $c_{NCO,0}$ and finally the initial molar concentration of water is $c_{W,0}$. R is the universal gas constant and T is the absolute temperature of the system.

The progress of the reaction between isocyanate and water to produce CO_2 (i.e., the blowing reaction), is monitored by the conversion of water, X_W:

$$\frac{\partial}{\partial t}\left(\alpha_f \rho_f X_W\right) + \nabla \cdot \left(\alpha_f \rho_f X_W \mathbf{U}\right) = \alpha_f \rho_f S_W \qquad \text{Eq. 4}$$

180 The source term for the blowing reaction is written in Eq. 5 where, in analogy with Eq. 3, A_W, and E_W
181 are the pre-exponential factor and the activation energy for the blowing reaction, respectively.

$$S_W = A_W \exp\left(-\frac{E_W}{RT}\right)(1 - X_W) \qquad \text{Eq. 5}$$

182 Additionally, the macro-scale CFD model should account for the amount of gas, L_{gas}, generated by the
183 evaporation of the physical blowing agent. The variable L_{gas} represents the mass fraction of physical
184 blowing agent with respect to the reacting liquid of the foam and it is obtained by solving Eq. 6,

$$\frac{\partial}{\partial t}\left(\alpha_f \rho_f L_{gas}\right) + \nabla \cdot \left(\alpha_f \rho_f L_{gas} \mathbf{U}\right) = \alpha_f \rho_f S_{BA} \qquad \text{Eq. 6}$$

185 where the source term is expressed as:

$$S_{BA} = \begin{cases} \dfrac{dL_{gas}}{dt} = \dfrac{dL_{gas}}{dT}\dfrac{dT}{dt} + \dfrac{dL_{gas}}{dp}\dfrac{dp}{dt} & if\ L_0 \geq L_{max}(p,T) \\ \dfrac{dL_{gas}}{dt} = 0 & if\ L_0 < L_{max}(p,T) \end{cases} \qquad \text{Eq. 7}$$

186 where L_0 is the mass fraction of physical blowing agent in the liquid of foam before foaming. It is worth
187 noting that the pressure changes with time is insignificant. Also, another simplifying assumption is that
188 the process is controlled by kinetics and the bubble scale phenomena such as nucleation and species
189 diffusion are not included in the modeling framework. In other words, the initial amount of blowing
190 agent is soluble in the reacting mixture and it immediately evaporates once it reaches the
191 supersaturated concentration in the mixture. This could be remedied by integrating a meso-scale model
192 for bubbles growth due to evaporation of blowing agents into this modeling platform, an example of
193 such an approach is presented elsewhere (Ferkl et al., 2016).

In order to close Eq. 6 and Eq. 7, the functional form of the solubility of the physical blowing agent in the liquid mixture should be clarified (i.e., $L_{max} = f(p,T)$). In our previous works (Ferkl et al., 2016; Karimi and Marchisio, 2015), we applied empirical correlations to relate the solubility to the absolute temperature of the system. However, in the current work surrogate models obtained from molecular dynamics data replace this assumption.

Moreover, the temperature evolution of the foam due to the endothermic and exothermic reactions is calculated by solving the following equation:

$$\frac{\partial T}{\partial t} + \nabla \cdot (T\mathbf{U}) - \nabla^2(\bar{\alpha}T) = \frac{\alpha_f}{\rho_{PU} c_f}\left[-\Delta H_W c_{W,0} \frac{DX_W}{Dt} - \Delta H_{OH} c_{OH,0} \frac{DX_{OH}}{Dt} + \rho_{PU}\Lambda \frac{DL_{gas}}{Dt}\right] \quad \text{Eq. 8}$$

In Eq. 8, $\bar{\alpha}$ is the thermal diffusivity adopted from (Geier et al., 2009). ΔH_W and ΔH_{OH} are the heat of reactions for the gelling and blowing reactions, Λ is the latent heat of the evaporation of physical blowing agent, c_f is the specific heat of the PU foam, and ρ_{PU} is the density of reaction mixture.

Knowing the kinetics of reactions and the absolute temperature, the PU foam density evolution can be formulated depending on the amount of different gases being produced due to the blowing reaction and evaporation of the physical blowing agent:

$$\rho_f = \left(1 + x_{W,0} + L_0\right) \times \left[\left(\frac{x_{W,0} X_W M_{CO_2}}{\rho_{PU}} - X_{eq}^{CO_2}\right)\frac{RT}{pM_{CO_2}} + \frac{(1 - X_W)x_{W,0}}{\rho_W} + \frac{L_{gas}RT}{pM_{BA}} + \frac{\left(L_0 - L_{gas}\right)}{\rho_{BA}} + \frac{1}{\rho_{PU}}\right]^{-1} \quad \text{Eq. 9}$$

Initial weight fractions of water and PBA in Eq. 9 are denoted as $x_{W,0}$, and L_0, whereas their molecular weights are M_{H_2O} and M_{BA}, respectively and M_{CO_2} is the molecular weight of carbon dioxide. The term p is the system pressure and ρ_{BA} defines the density of the physical blowing agent in the liquid. Finally, $X_{eq}^{CO_2}$ indicates the equilibrium weight fraction of carbon dioxide in the liquid mixture. Eq. 9 contains two properties that can be accurately estimated by using MD data. Specifically, the equilibrium weight fraction of carbon dioxide in the liquid mixture ($X_{eq}^{CO_2}$) and the density of the reacting mixture (ρ_{PU}), which were previously assumed to be constant, can be estimated by molecular simulations. However, as already mentioned above, in this work we adopt a more sophisticated approach by further deriving the dependence of these two quantities on temperature and degree of cross-linking via computational chemistry.

The macro-scale model is also equipped with a non-Newtonian rheology model based on the Bird-Carreau equation (Byron Bird and Carreau, 1968). In the present formulation, the dependency of the foam apparent viscosity on temperature, conversion of hydroxyl group, and shear rate ($\dot{\gamma}$) is accounted for as:

$$\mu_{app} = \mu_\infty + (\mu_0 - \mu_\infty)[1 + (\lambda\dot{\gamma})^2]^{\frac{n-1}{2}} \qquad \text{Eq. 10}$$

The zero-shear (μ_0) and the infinite-shear (μ_∞) foam viscosities are represented as:

$$\mu_0 = \left[\ln(d + X_{OH}) - \ln(d) + \left(\frac{X_{OH,gel}}{X_{OH,gel} - X_{OH}}\right)^{a+bX_{OH}+cX_{OH}^2}\right]\mu_{0,L} \qquad \text{Eq. 11}$$

$$\mu_\infty = \left[\ln(d + X_{OH}) - \ln(d) + \left(\frac{X_{OH,gel}}{X_{OH,gel} - X_{OH}}\right)^{a+bX_{OH}+cX_{OH}^2}\right]\mu_{\infty,L} \qquad \text{Eq. 12}$$

where $X_{OH,gel}$ is the gelling point and the model parameter values are: $a = 1.5$, $b = 1.0$, $c = 0.0$, $d = 0.001$, $\lambda = 11.35$, $n = 0.2$, $\mu_{0.L} = 0.195$, and $\mu_{\infty.L} = 0.266$, respectively. These model constants are here taken from previous empirical works in this area (Winkler, 2009). Also for the calculation of these parameters a multiscale modeling approach could be formulated. This is the focus of our current work and will be reported in future communications.

3. Scale coupling, test cases and operating conditions

Figure 1 and Figure 2 together with Table 1 and Table 2 summarize the MD data, the surrogate models and the relevant parameter values obtained for the first chemical recipe.

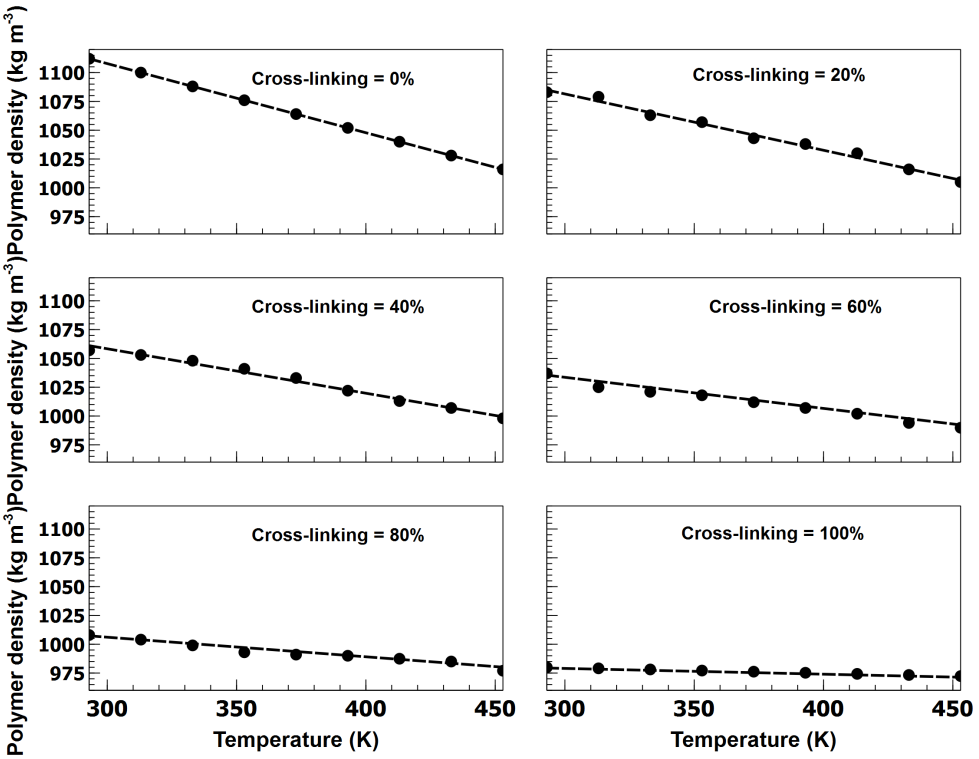

Figure 1. Molecular dynamics data (symbols) and relevant surrogate models implemented in the CDF code (dotted lines) for polymer density based on molecular dynamics data under different degree of PU cross-linking.

Cross linking (%)	Surrogate model	Model constants
0	$\rho_{PU} = a \times T + b$	$a = -0.6, \quad b = 1287.8$
20		$a = -0.5, \quad b = 1228.1$
40		$a = -0.4, \quad b = 1174.1$
60		$a = -0.3, \quad b = 1114.6$
80		$a = -0.2, \quad b = 1057.1$
100		$a = -0.05, \quad b = 994.0$

Table 1. Surrogate model and relevant parameters for polymer density at different degree of PU cross-linking.

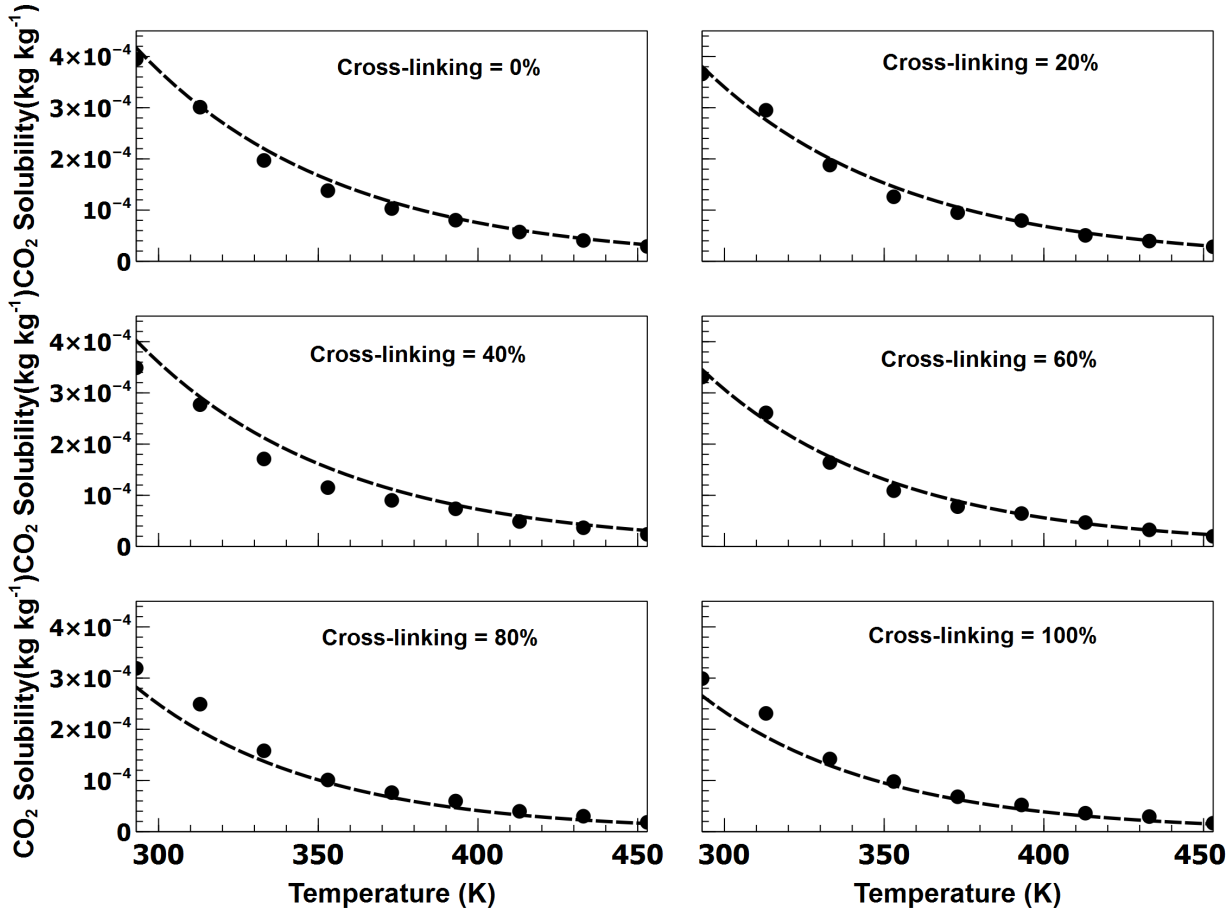

Figure 2. Molecular dynamics data (symbols) and relevant surrogate models (dotted lines) implemented in the CFD code for solubility of carbon dioxide based on molecular dynamics data under different degree of PU cross-linking.

Cross linking (%)	Surrogate model	Model constants
0	$X_{eq}^{CO_2} = a \times \exp(-bT)$	$a = 0.0453, \quad b = 0.016$
20		$a = 0.0413, \quad b = 0.016$
40		$a = 0.0437, \quad b = 0.016$
60		$a = 0.0503, \quad b = 0.017$
80		$a = 0.0551, \quad b = 0.018$
100		$a = 0.0518, \quad b = 0.018$

Table 2. Surrogate model and relevant parameters for solubility of carbon dioxide at different degree of PU cross-linking.

230

231 As can be seen from Figures 1 and 2, MD simulations predict that both the density of the polymerizing
232 mixture and the solubility of carbon dioxide in the reacting mixture decrease with increasing
233 temperature and degree of cross-linking, as somewhat expected.

234 The second recipe includes both CBA and PBA. In this case, water and n-pentane cause the foam to
235 expand due to the concomitant generation of carbon dioxide and the evaporation of physical blowing
236 agent. Therefore, besides the solubility of CO_2, the solubility of n-pentane (L_{max} in Eq. 7), calculated
237 from the MD simulations for different temperatures and cross-linking levels, should be fed into the CFD
238 code via the relevant surrogate models. Figure 3 and Table 3 show the MD results, their fitting by
239 surrogate models, and the relevant model parameters for n-pentane at different degrees of PU
240 polymerization. Also in this case MD predictions are sensible and yield the expected qualitative
241 behavior. The paramount importance of these predictions, however, is that they provide quantitative
242 estimates whose accuracy will be discussed later when the comparison with experiment is presented.

243
244

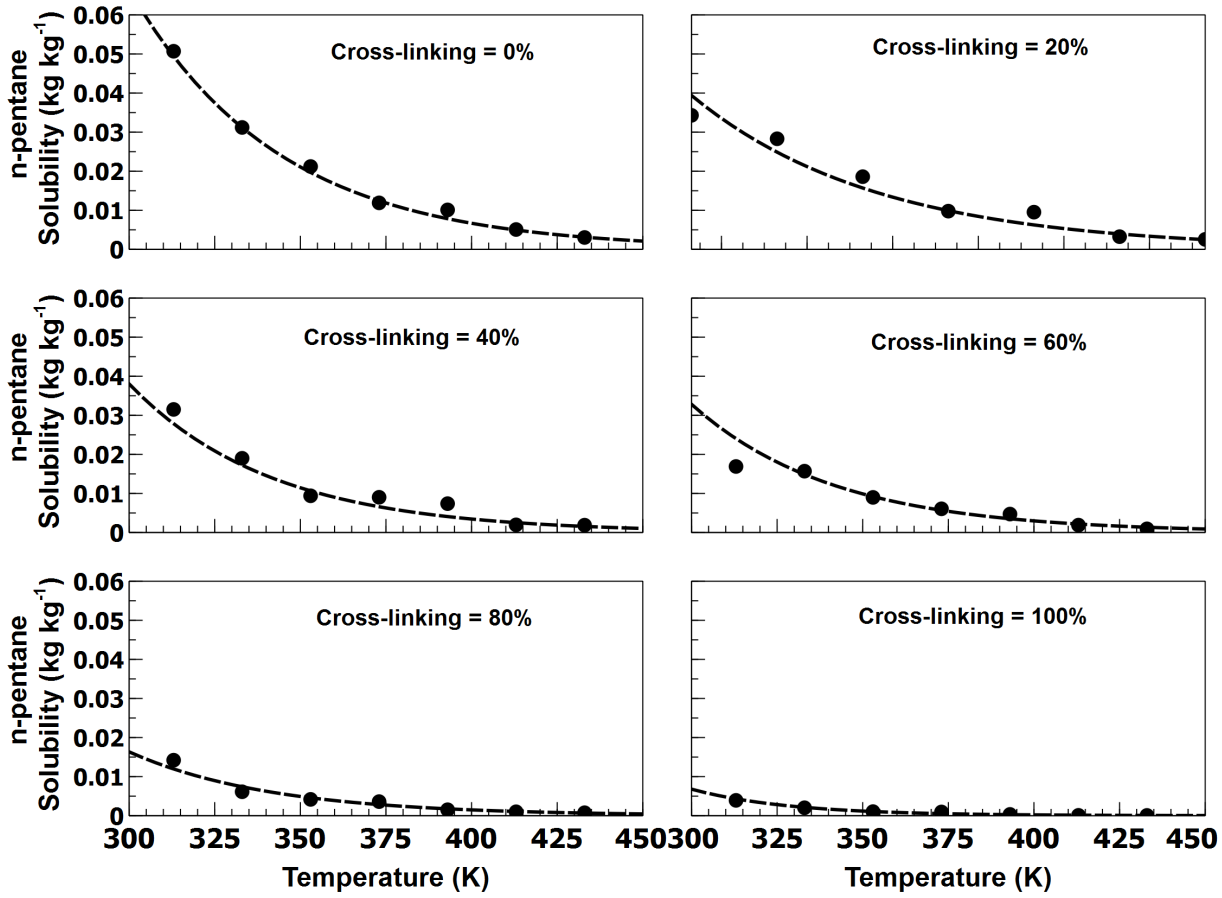

Figure 3. Molecular dynamics data and surrogate models for solubility of n-pentane based on molecular dynamics data under different degree of PU cross-linking. Symbols: MD data; dotted line: corresponding surrogate model implemented in the CFD code.

Cross linking (%)	Surrogate model	Model constants
0	$L_{max} = a \times \exp(-bT)$	$a = 66.089,\quad b = 0.023$
20		$a = 52.710,\quad b = 0.023$
40		$a = 50.942,\quad b = 0.024$
60		$a = 43.963,\quad b = 0.024$
80		$a = 21.878,\quad b = 0.024$
100		$a = 246.51,\quad b = 0.035$

Table 3. Surrogate model and relevant parameters for solubility of n-pentane at different degree of PU cross-linking.

The initial concentrations of different reactants and the kinetic properties for the different PU foam batches simulated in this work are described in Table 4 and 5.

Recipe	Batch	$c_{OH,0}$ (mol m^{-3})	$c_{NCO,0}$ (mol m^{-3})	$c_{W,0}$ (mol m^{-3})	L_0 (kg kg^{-1})
	a	4400	4400	305	-
1	b	4400	4400	610	-
	c	4400	4400	915	-
2	d	5140	4455	671	0.057

Table 4. Summary of the initial conditions adopted for the 4 PU foam batches investigated.

Batch	A_{OH} (m^3 mol^{-1} s^{-1})	E_{OH} (J mol^{-1})	$-\Delta H_{OH}$ (J mol^{-1}K^{-1})	A_W (s^{-1})	E_W (J mol^{-1})	$-\Delta H_W$ (J mol^{-1}K^{-1})
a - c	1.735	4.04×10^4	7.07×10^4	1390	3.37×10^4	8.60×10^4
d	1.0	3.15×10^4	6.85×10^4	1050	2.70×10^4	8.15×10^4

Table 5. Summary of the kinetics parameters for the 4 PU batches in Table 4.

The transient CFD simulations are carried out for the classical "mixing cup" experiment using ANSYS Fluent 15.0 VOF approach to handle the interface between the two phases. The cup is represented as a two-dimensional (2D) planar test case with structured meshes. The first 10% of computational domain is filled by the liquid mixture with the initial amount of gases (i.e., CO_2 and evaporated blowing agent) set to zero. These settings have been selected with a two-fold purpose: to mimic the experimental conditions adopted by Baser and Khakhar (S. A. Baser and Khakhar, 1994; S A Baser and Khakhar, 1994) and validate the foam density and temperature evolutions against their measurements. The pressure-outlet boundary condition is prescribed for the top part of the domain, while the other sides are assumed to be walls. Further, four additional User Defined Scalars (UDSs) are defined to evaluate the polymerization progress (i.e., Eq. 2, Eq. 4, and Eq. 6) and the temperature evolution (i.e., Eq. 8) of the foam phase. The corresponding source terms (i.e., Eq. 3, Eq. 5, Eq. 7, and Eq. 8) are also coded as User Defined Functions (UDFs). Moreover, the PU foam material properties such as density and apparent viscosity are calculated using the `DEFINE_PROPERTY` macro available in ANSYS Fluent. It is worth pointing out that the different surrogate models are incorporated into the UDF to evaluate the CFD requirements (i.e., density of reacting mixture, solubility of CO_2, and solubility of n-pentane) for

different temperature and cross-linking. A linear relationship between the degree of cross-linking and conversion of the hydroxyl group, X_{OH} is assumed. In particular, we assume that when X_{OH} is equal to zero also the degree of cross-linking is equal to 0%. When X_{OH} is instead equal to the maximum value, corresponding to the gelling point (i.e. $X_{OH} = 0.6$), the degree of cross-linking is taken equal to 100%. The surrogate model is therefore linearly interpolating between these minimum and maximum values.

The governing equations are discretized by using the first-order upwind discretization scheme, while CICSAM is applied for the reconstruction of the interface between the foam and the surrounding air. The convergence is determined by monitoring the residuals of continuity, velocities, and UDSs equations. A converged solution is achieved when all the residuals fall below 1×10^{-3}.

4. Results and discussion

The final application of the multiscale simulation suite developed in this work was to monitor the PU foam expansion during mold filling. Thus, the preliminary observation focused on how the model handles foam expansion. Figure 4 displays the volume fraction of surrounding air at four different time instants. The simulation represents batch d in Table 4, including n-pentane as PBA and water as CBA. As explained in the previous section, the first 10% of beaker is filled with the foam phase at the beginning of simulation (see Figure 4 at time = 1s). At the second time instance, when the blowing reaction results in the production of carbon dioxide, foam expansion begins. By increasing temperature, n-pentane reaches its equilibrium value and contributes to foam expansion by evaporation. This phenomenon can be seen in the last two snapshots, where foam expansion accelerates due to the large presence of evaporated PBA.

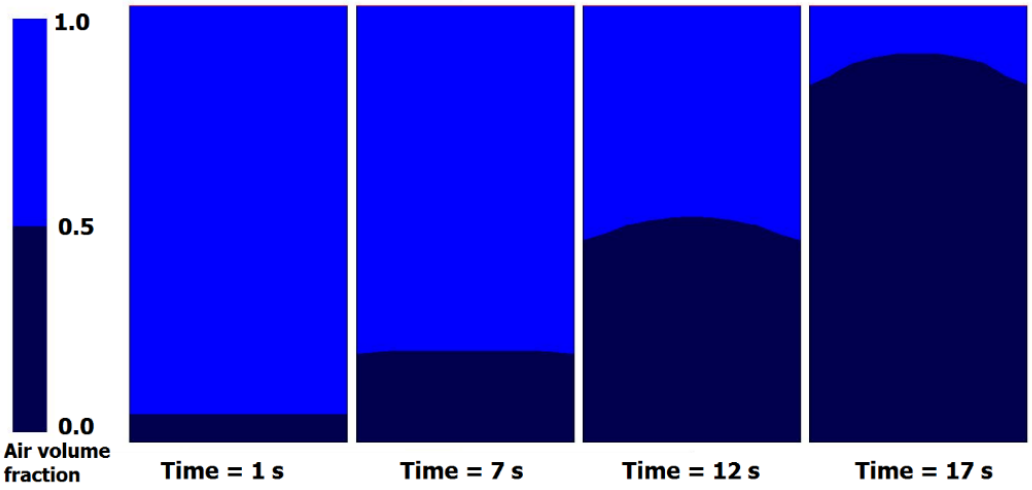

Figure 4. PU foam expansion profile for batch d.

Figure 5 shows the time evolution of foam apparent density for the four batches investigated. As seen from all panels in Figure 5, for all test cases the time profile of the density has been captured correctly, in that the density decreases from its initial values corresponding to that of the liquid mixture and eventually levels off to its final value. For batch d, due to the presence of physical blowing agent the density evolution occurs faster compared to the other batches. As seen in the corresponding panel of Figure 5, the system density reaches its final value just after 30 seconds of polymerization while, for the other cases in which only the chemical blowing agent is present, the same condition is reached after approximately 250 seconds. This trend is also confirmed by the data in Figure 4, for which the fast expansion of batch d is observed. It is noteworthy to highlight the influence of water content in Recipe 1. This is directly reflected on the final density of the foam which, in turn, determines the final properties of the product. For example, at 250 seconds of simulation, the foam apparent density for batch a with $c_{W,0}$ = 305 mol m^{-3} is 138 kg m^{-3}, whereas increasing the amount of water for batch b and c to $c_{W,0}$ = 610 mol m^{-3} and $c_{W,0}$ = 915 mol m^{-3} respectively, results in the final densities of 51 kg m^{-3} and 34 kg m^{-3}. The pattern observed implies that the modeling tool converges the amount of gas being produced during the polymerization into the foam density. In other words, higher amount of water in the recipe yields more CO_2 in the system and this ultimately results in lower-density PU foams.

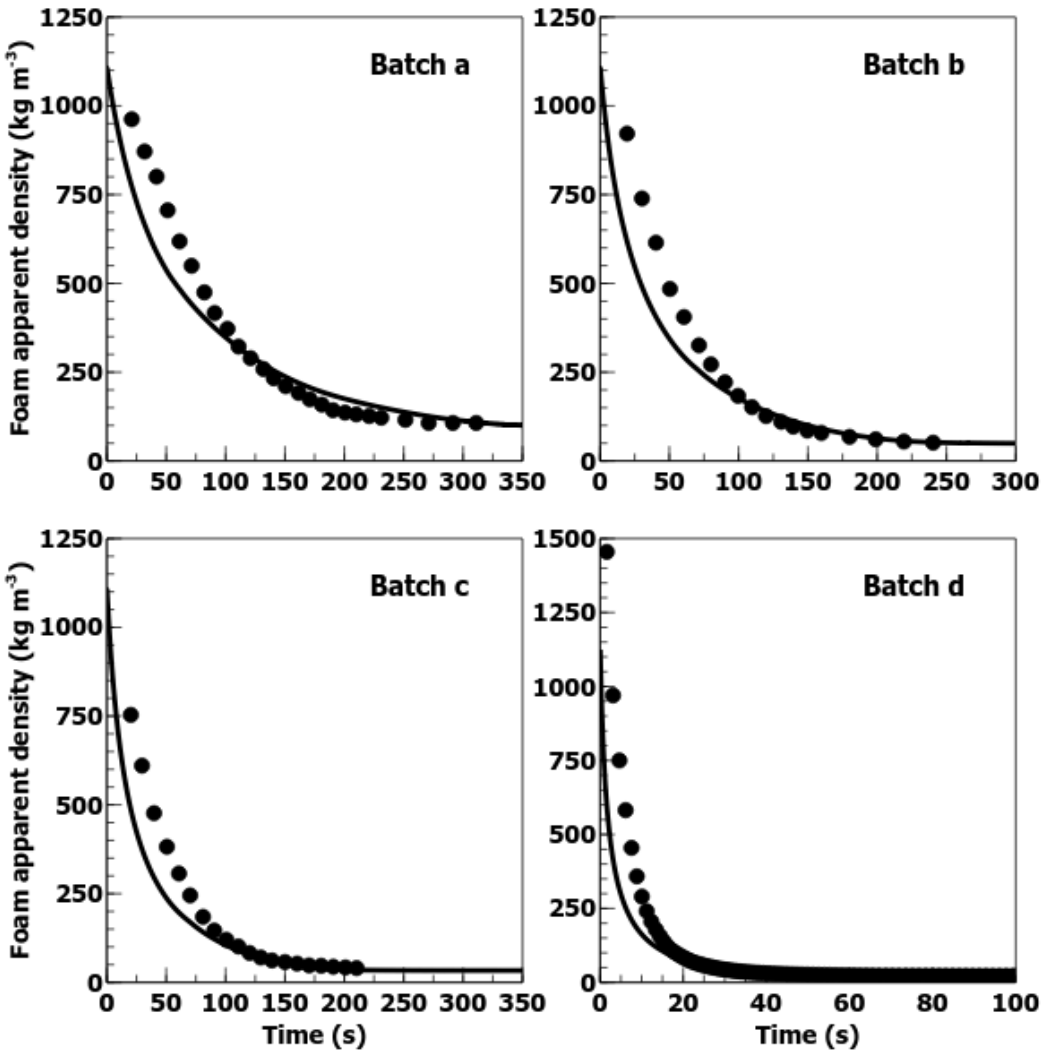

Figure 5. Numerical predictions of PU foam density for batches a-d as a function of time (solid-line) compared with experimental data (symbols).

306 Figure 6 shows the comparison between numerical predictions and experimental data for the foam
307 temperature as a function of time: the nice qualitative agreement between the two data sets further
308 supports the ability of the proposed multiscale model in correctly predicting the PU-based foaming
309 process. Besides the fast expansion for batch d, comparison of the temperature trend between this
310 batch and the chemically blown batches show that at invariant times the temperature is lower for the
311 physically blown foam. This is attributed to the consumption of heat during the evaporation of physical
312 blowing agent. The amount of water in Recipe 1 also affects the temperature. In that, increasing the

concentration of water in the mixture increases the temperature. As a case in point, after 250 seconds of foaming for batches a, b, and c the absolute temperatures of the foam phase are 366 K, 417 K, and 426 K, respectively. Basically, this indicates the intensity of the exothermic blowing reaction and the higher production of heat in the presence of more water. Overall the comparison leads to reasonable agreement, that could be improved if more detailed thermal conductivity and heat capacity models for the PU foam were used (Geier et al., 2009).

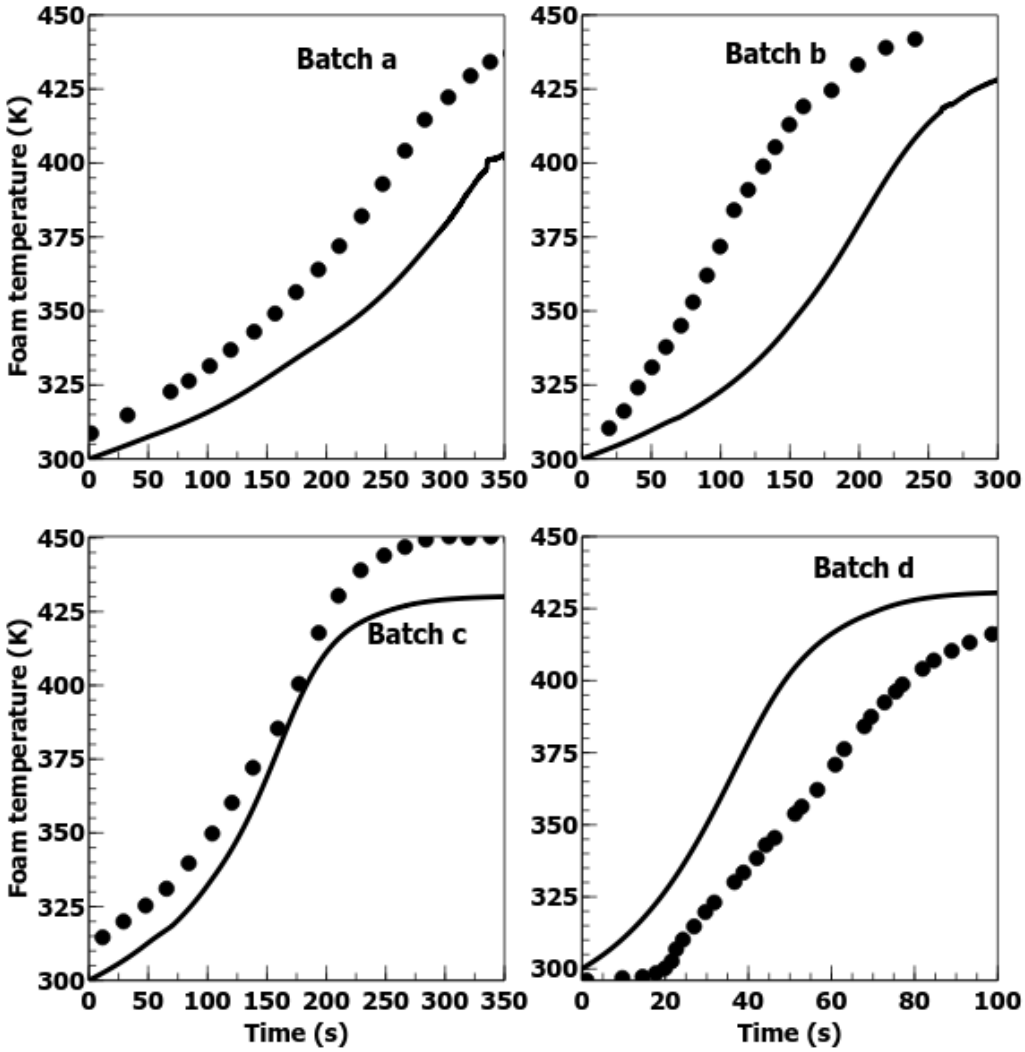

Figure 6. Numerical predictions of foam temperature as a function of time (solid-line) with experimental data (symbols).

5. Conclusions

A multi-scale modeling approach is introduced in this work for the simulation of the expansion of PU foams. The model is formulated by coupling a nano-scale model, based on MD, with a macro-scale model, based on VOF and CFD. The lower scale model provides the inputs of the CFD code including the density of polymerizing liquid mixture and the solubility of blowing agents (chemical and physical). The functionality of the CFD inputs on temperature and cross linking are also accounted for using the surrogate model concept. The multi-scale modeling strategy is tested and validated for two PU recipes in which water and n-pentane are used as chemical and physical blowing agents. The reasonable level of agreement achieved in both cases shows that not only the developed approach offers an efficient method of linking between the two modeling tools, but it also provides accurate numerical predictions of PU foam properties. This work will continue to incorporate detailed models for the kinetics of reactions as well foam rheology.

6. Acknowledgements

This work was funded by the European Commission under the grant agreement number 604271 (Project acronym: MoDeNa; call identifier: FP7-NMP-2013-SMALL-7). Computational resources were provided by HPC@POLITO, a project of Academic Computing within the Department of Control and Computer Engineering at the Politecnico di Torino (http://hpc.polito.it).

7. References

Baser, S.A., Khakhar, D. V., 1994. Modeling of the Dynamics of Water and R-11 blown polyurethane foam formation. Polym. Eng. Sci. 34, 642–649. doi:10.1002/pen.760340805

Baser, S.A., Khakhar, D. V, 1994. Modeling of the Dynamics of R-11 Blown Polyurethane Foam Formation. Polym. Eng. Sci. 34, 632–641. doi:10.1002/pen.760340805

Bikard, J., Bruchon, J., Coupez, T., Vergnes, B., 2005. Numerical prediction of the foam structure of polymeric materials by direct 3D simulation of their expansion by chemical reaction based on a multidomain method. J. Mater. Sci. 40, 5875–5881. doi:10.1007/s10853-005-5022-9

Byron Bird, R., Carreau, P.J., 1968. A nonlinear viscoelastic model for polymer solutions and melts—I. Chem. Eng. Sci. 23, 427–434. doi:10.1016/0009-2509(68)87018-6

Cosoli, P., Ferrone, M., Pricl, S., Fermeglia, M., 2008a. Hydrogen sulphide removal from biogas by zeolite adsorptionPart I. GCMC molecular simulations. Chem. Eng. J. 145, 86–92. doi:10.1016/j.cej.2008.07.034

Cosoli, P., Ferrone, M., Pricl, S., Fermeglia, M., 2008b. Hydrogen sulfide removal from biogas by zeolite adsorption. Part II. MD simulations. Chem. Eng. J. 145, 93–99. doi:10.1016/j.cej.2008.08.013

Cosoli, P., Scocchi, G., Pricl, S., Fermeglia, M., 2008. Many-scale molecular simulation for ABS–MMT nanocomposites: Upgrading of industrial scraps. Microporous Mesoporous Mater. 107, 169–179. doi:10.1016/j.micromeso.2007.03.017

Feng, J.J., Bertelo, C.A., 2004. Prediction of bubble growth and size distribution in polymer foaming based on a new heterogeneous nucleation model. J. Rheol. (N. Y. N. Y). 48, 439–462. doi:10.1122/1.1645518

Ferkl, P., Karimi, M., Marchisio, D.L., Kosek, J., 2016. Multi-scale modelling of expanding polyurethane

foams: Coupling macro- and bubble-scales. Chem. Eng. Sci. 148, 55–64. doi:10.1016/j.ces.2016.03.040

Ferkl, P., Toulec, M., Laurini, E., Pricl, S., Fermeglia, M., Auffarth, S., Eling, B., Settels, V., Kosek, J., 2017. Multi-scale modelling of heat transfer in polyurethane foams. Chem. Eng. Sci. 172, 323–334. doi:10.1016/j.ces.2017.06.035

Fermeglia, M., Pricl, S., 2007. Multiscale modeling for polymer systems of industrial interest. Prog. Org. Coatings 58, 187–199. doi:10.1016/j.porgcoat.2006.08.028

Fermeglia, M., Pricl, S., 1999a. A novel approach to thermophysical properties prediction for chloro-fluoro-hydrocarbons. Fluid Phase Equilib. 166, 21–37. doi:10.1016/S0378-3812(99)00295-2

Fermeglia, M., Pricl, S., 1999b. Molecular dynamics simulations of real systems: application to chloro-fluoro-hydrocarbons and polymers. Fluid Phase Equilib. 158–160, 49–58. doi:10.1016/S0378-3812(99)00093-X

Fermeglia, M., Pricl, S., 1999c. Equation-of-state parameters for pure polymers by molecular dynamics simulations. AIChE J. 45, 2619–2627. doi:10.1002/aic.690451218

G. Harikrishnan, T. Umasankar Patro, and, Khakhar*, D. V., 2006. Polyurethane Foam−Clay Nanocomposites: Nanoclays as Cell Openers. doi:10.1021/IE0600994

Geier, S., Winkler, C., Piesche, M., 2009. Numerical Simulation of Mold Filling Processes with Polyurethane Foams. Chem. Eng. Technol. 32, 1438–1447. doi:10.1002/ceat.200900202

Gupta, V.K., Khakhar, D. V., 1999. Formation of integral skin polyurethane foams. Polym. Eng. Sci. 39, 164–176. doi:10.1002/pen.11405

Harikrishnan, G., Khakhar, D. V., 2009. Modeling the dynamics of reactive foaming and film thinning in polyurethane foams. AIChE J. 56, NA-NA. doi:10.1002/aic.12002

383 Karimi, M., Droghetti, H., Marchisio, D.L., 2016. Multiscale Modeling of Expanding Polyurethane Foams
384 via Computational Fluid Dynamics and Population Balance Equation. Macromol. Symp. 360, 108–
385 122. doi:10.1002/masy.201500108

386 Karimi, M., Marchisio, D.L., 2015. A Baseline Model for the Simulation of Polyurethane Foams via the
387 Population Balance Equation. Macromol. Theory Simulations 24, 291–300.
388 doi:10.1002/mats.201500014

389 Kim, C., Youn, J.R., 2000. Environmentally Friendly Processing of Polyurethane Foam for Thermal
390 Insulation. Polym. Plast. Technol. Eng. 39, 163–185. doi:10.1081/PPT-100100022

391 Larsen, G.S., Lin, P., Hart, K.E., Colina, C.M., 2011. Molecular Simulations of PIM-1-like Polymers of
392 Intrinsic Microporosity. Macromolecules 44, 6944–6951. doi:10.1021/ma200345v

393 Laurini, E., Posocco, P., Fermeglia, M., Pricl, S., 2016. MoDeNa Nanotools: An integrated multiscale
394 simulation workflow to predict thermophysical properties of thermoplastic polyurethanes. J.
395 Comput. Sci. 15, 24–33. doi:10.1016/j.jocs.2015.11.006

396 Maly, M., Posocco, P., Fermeglia, M., Pricl, S., 2008. Scripting approach in hybrid organic–inorganic
397 condensation simulation: the GPTMS proof-of-concept. Mol. Simul. 34, 1215–1236.
398 doi:10.1080/08927020802235706

399 Mensitieri, G., Larobina, D., Guerra, G., Venditto, V., Fermeglia, M., Pricl, S., 2008. Chloroform sorption
400 in nanoporous crystalline and amorphous phases of syndiotactic polystyrene. J. Polym. Sci. Part B
401 Polym. Phys. 46, 8–15. doi:10.1002/polb.21303

402 Mills, N.J., 1993. Handbook of polymeric foams and foam technology. Polymer (Guildf). 34, 2237.
403 doi:10.1016/0032-3861(93)90758-3

404 Milocco, O., Fermeglia, M., Pricl, S., 2002. Prediction of thermophysical properties of alternative

refrigerants by computational chemistry. Fluid Phase Equilib. 199, 15–21. doi:10.1016/S0378-3812(01)00811-1

Pricl, S., Fermeglia, M., 2003. Atomistic molecular dynamics simulations of gas diffusion and solubility in rubbery amorphous hydrocarbon polymers. Chem. Eng. Commun. 190, 1267–1292. doi:10.1080/00986440302153

Princen, H.M., Kiss, A.D., 1986. Rheology of foams and highly concentrated emulsions. J. Colloid Interface Sci. 112, 427–437. doi:10.1016/0021-9797(86)90111-6

Samkhaniani, N., Gharehbaghi, A., Ahmadi, Z., 2013. Numerical simulation of reaction injection molding with polyurethane foam. J. Cell. Plast. 49, 405–421. doi:10.1177/0021955X13485594

Scocchi, G., Paola, P., Maurizio, F., Pricl, S., 2007a. Polymer−Clay Nanocomposites: A Multiscale Molecular Modeling Approach. J. Phys. Chem. B 111, 2143–2151. doi:10.1021/JP067649W

Scocchi, G., Posocco, P., Danani, A., Pricl, S., Fermeglia, M., 2007b. To the nanoscale, and beyond! Fluid Phase Equilib. 261, 366–374. doi:10.1016/j.fluid.2007.07.046

Scocchi, G., Posocco, P., Handgraaf, J.-W., Fraaije, J.G.E.M., Fermeglia, M., Pricl, S., 2009. A Complete Multiscale Modelling Approach for Polymer-Clay Nanocomposites. Chem. - A Eur. J. 15, 7586–7592. doi:10.1002/chem.200900995

Seo, D., Ryoun Youn, J., Tucker, C.L., 2003. Numerical simulation of mold filling in foam reaction injection molding. Int. J. Numer. Methods Fluids 42, 1105–1134. doi:10.1002/fld.582

Seo, D., Youn, J.R., 2005. Numerical analysis on reaction injection molding of polyurethane foam by using a finite volume method. Polymer (Guildf). 46, 6482–6493. doi:10.1016/j.polymer.2005.03.126

Sun, H., 1998. COMPASS: An ab Initio Force-Field Optimized for Condensed-Phase ApplicationsOverview

with Details on Alkane and Benzene Compounds. doi:10.1021/JP980939V

Toth, R., Santese, F., Pereira, S.P., Nieto, D.R., Pricl, S., Fermeglia, M., Posocco, P., 2012. Size and shape matter! A multiscale molecular simulation approach to polymer nanocomposites. J. Mater. Chem. 22, 5398. doi:10.1039/c2jm15763b

Ubbink, O., 1997. Numerical prediction of two fluid systems with sharp interfaces. Imperial College of Science, Technology & Medicine.

Winkler, C., 2009. Numerische und experimentelle Untersuchungen zu Formfllvorgngen mit Polyurethanschumen unter komplexen Randbedingungen. University of Stuttgart.

Woods, G., 1990. The ICI polyurethanes book, Second. ed. ICI Polyurethanes and Wiley, New York.